Experimental and Analytical Study Approach of Artificial Basilar Membrane Prototype (ABMP)

Harto Tanujaya[1], Hirofumi Shintaku[3], Dai Kitagawa[3], Adianto[1], Susilodinata[2] & Satoyuki Kawano[3]

[1]Mechanical Engineering Department, Faculty of Engineering, Tarumanagara University, Jalan Letjen. S. Parman No. 1, Jakarta 11440, Indonesia
[2]Faculty of Medicine, Tarumanagara University, Jalan Letjen. S. Parman No. 1, Jakarta 11440, Indonesia
[3]Mechanical Science and Bioengineering Department, Graduate School of Engineering Science, Osaka University, Machikaneyama-cho 1-3, Toyonaka, Osaka 560-8531, Japan
Email: hart_tan18@yahoo.com

Abstract. In this research, we have developed, fabricated, tested, and analyzed an artificial basilar membrane prototype (ABMP), which works using sinusoidal waves of various frequencies. The design of the prototype has a trapezoidal shape with a length of 30 mm and a width of 2 to 4 mm. The research was carried out experimentally and analytically. Experimentally, the ABMP's vibration was measured using a laser Doppler vibrometer (LDV) and a function generator to generate various frequencies. The analytical approach is discussed based on the Wentzel Kramer Brillouin method (WKB). The results show that resonance frequencies can be reached within the range of human hearing, between 20 Hz to 20 kHz.

Keywords: *ABMP; cochlea; frequency; frequency selectivity; PVDF; resonance; vibrating amplitude; WKB.*

1 Introduction

The ears are a component of the human auditory system. Hearing impairment can be brought about by many causes. Sensorineural hearing loss is one of them. Usually, in medicine a cochlear implant (CI) or hearing aid (HA) is used to assist the patient who suffers from deafness. In this paper, we discuss an artificial basilar membrane prototype (ABMP) using a piezoelectric membrane made of polyvinylidene fluoride (PVDF). The function of the cochlea in the human auditory system is not only to convert acoustic sound to electrical signals but also frequency selectivity. The biological basilar membrane, which is a resonator in the cochlea, plays a prominent role infrequency selectivity. In this experiment, we report the development of a fully self-contained artificial cochlea, the aforementioned ABMP. The acoustic sensor which is reported in this paper realizes frequency selectivity in the air. Normal humans can hear sounds in the frequency range of 20 Hz to 20 kHz.

Received on August 8th, 2011, 1st Revision on November 3rd, 2011, 2nd Revision May 2nd, 2012, 3rd Revision May 24th, 2012, 4th Revision January 15th, 2013, Accepted for publication January 21st, 2013.
 ISSN: 2337-5779, DOI: 10.5614/j.eng.technol.sci.2013.45.1.5

2 Mechanical Model

For modeling purposes and in order to simplify the model of the biological basilar membrane, the ABMP can be unwrapped. There are two channels above and below the ABMP, as shown in Figure 1(a). The channels are considered as the scala vestibule and the scala tympaniin the biological cochlea. Figure 1(a) shows the complete geometry of the ABMP model, from the top and through its cross section. This condition is made for the analytical calculation. Figure 1(b) shows a 3D view of the ABMP that was used in our experiment.

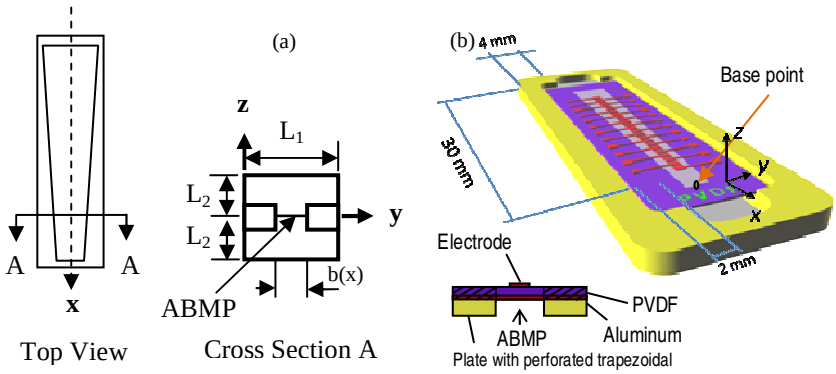

Figure 1 Geometric model of artificial basilar membrane prototype (ABMP), (a) top and cross section view, (b) 3D view.

The ABMP is made of PVDF membrane and is bonded on a stainless steel plate, which has a trapezoidal shaped perforation with a width ranging from 2 mm to 4 mm and a length of 30 mm. The thickness of the ABMP is 40 μm. There are 24 detecting electrodes on the ABMP, which are fabricated using photolithograpy and etching. The whole array of detecting electrodes is made of aluminium thin film with a thickness of 500 nm and they are located on the central line of the trapezoidal shape. The Young modulus and density of the membrane are 4 GPa and 1790 kg/m3 respectively. The membrane and the perforated trapezoid are mounted on a substrate with a channel. The channel's dimensions are 47 × 17 mm (rectangular) and a depth of 4 mm, as shown in Figure 1(b).

3 Analytical Approach

Many researchers have analyzed the theory of the cochlea. Von Bekesy [1] analyzed a mechanical cochlea to study the traveling wave. Steele & Taber [2] analyzed and constructed a mechanical cochlear model using a three-dimensional model. Zhou, *et al.* [3] used an isotropic polymer membrane placed

on a plate to build the first life-sized mechanical cochlea. Kirchhoff's hypotheses are fundamental assumptions for the development of linear, elastic, small-deflection theories concerning the bending of thin plates [4]. Thin plate bending theory usually refers to Kirchhoff's plate theory. The method of Wentzel Kramer Brillouin (WKB) was also used to solve the equations of the mechanism of the membrane problem, whereby the parameters are very slowly compared to the wavelength of the oscillations. The solution of the vibration of the membrane response is assumed with a slowly varying amplitude. Interaction between the fluid and the membrane is governed by linearized Euler equations.

In order to obtain the oscillatory solution at the steady state, some assumptions are made. The following assumptions are used to derive the basic equations of the ABMP. Vibration as a thin plate can be satisfied under the following conditions: deflections of the ABMP are very small compared to its thickness and the tensile term is negligible in the response of the structure. According to these assumptions, the ABMP is modeled as a thin bending plate, because the thickness of the membrane is extremely small compared to its width and length, and the plane stress is assumed to be $\sigma_z = \tau_{xz} = \tau_{yz} = 0$. Based on the shearing force and bending moment of the ABMP model, and the equation of motion, the governing equation of the bending vibration of the plate with isotropic mechanical properties can be described as,

$$D\left(\frac{\partial^4 w}{\partial x^4}+2\frac{\partial^2 w}{\partial x^2 \partial y^2}+\frac{\partial^4 w}{\partial y^4}\right)+\rho h\frac{\partial^2 w}{\partial t^2}=0 \tag{1}$$

where,

$$D = \frac{Eh^3}{12\left(1-\upsilon^2\right)} \tag{2}$$

E : Young Modulus
h : thickness of the membrane
ν : Poisson's ratio.

Problems for fluid structure interaction are relatively complex, so to obtain a mathematical solution, the following assumptions are made, based on the experimental observations. The ABMP can be unrolled in order to simplify the model and the vibration of the ABMP is modeled as the vibration of a thin plate with small bending amplitude; the fluid flow is assumed to be incompressible, and the gravity effects of the surrounding fluid were ignored. Furthermore, the following assumptions are made in order to obtain the oscillatory solution at the periodic steady state**.** A single mode $\eta(x, y)$ is used for the shape function of the

ABMP's bending in y direction. $\eta(x, y)$ is determined based on the analytical solution of a vibrating beam with the first mode, the length of $b(x)$, and the fixed boundary conditions at $y = \pm\frac{b(x)}{2}$ as,

$$\eta(x,y) = \begin{cases} c_1 \cos\left(\frac{\beta}{b(x)} y\right) + c_2 \cosh\left(\frac{\beta}{b(x)} y\right) & \text{at } -\frac{b(x)}{2} \le y \le \frac{b(x)}{2} \\ 0 & \text{at } -\frac{L_1}{2} \le y \le -\frac{b(x)}{2} \text{ and } \frac{b(x)}{2} \le y \le \frac{L_1}{2} \end{cases}, \quad (3)$$

where c_1, c_2, and β are constants, 0.8827, 0.1173 and 4.730, respectively, which are obtained and compared with the experimental results. These constants are determined so as to make $\eta(x,y)$ satisfy the fixed boundary conditions at $y = \pm b(x)/2$.

The wave is considered as a slowly varying wave in x direction [5]. That is, wave number $k(x)$ is slowly varying along x as $b(x)$, where $db(x)/dx \cong 0$ and $dk(x)/dx \cong 0$ are reasonable in the scale of one wavelength. In this case, the waves can be treated as pseudo plane waves and can be described by the WKB asymptotic solution [4]. Based on the assumptions described above, the displacement $w(x,y,t)$ of the ABMP can be written as

$$w = W(x)\eta(x, y)e^{i\int_0^x k(\xi)d\xi} e^{-i\omega t}, \quad (4)$$

where i and $W(x)$ are the imaginary number and the envelope function, respectively. $W(x)$ is also treated as a slowly varying function, that is $dW(x)/dx \cong 0$, since the effect of $dW(x)/dx$ on the dispersion relationship is trivial for linear problems. The basic equation of the fluid flow is the Laplace equation of velocity potential ϕ_f, written as

$$\frac{\partial^2 \phi_f}{\partial x^2} + \frac{\partial^2 \phi_f}{\partial y^2} + \frac{\partial^2 \phi_f}{\partial z^2} = 0. \quad (5)$$

The boundary conditions of the normal velocities at the wall of the fluid channel are written as

$$u_z = \frac{\partial \phi_l}{\partial z} = 0 \text{ at } z = -L_2, \quad (6)$$

$$u_{\mathrm{y}} = \frac{\partial \phi_l}{\partial y} = 0 \text{ at } y = \pm \frac{L_1}{2}, \tag{7}$$

The subscript f is u or l, where u and l indicate the fluid at the upper and lower sides of the ABMP, respectively. L_1 and L_2 are the width and the depth of the fluid channel, respectively. The kinematic boundary condition at z=0 is written as

$$\frac{\partial w}{\partial t} = \frac{\partial \phi_{\mathrm{f}}}{\partial \mathrm{z}} \text{ at } z = 0 \tag{8}$$

Therefore, the velocity potential can be written as

$$\phi_{\mathrm{l}} = \sum_{j=0}^{\infty} A_{\mathrm{j}} \cosh\left[\zeta_{\mathrm{j}}\left(z + L_2\right)\right] \cos\left(\frac{j\pi}{L_1} y\right) e^{i\int_0^x k(\xi)d\xi} e^{-i\omega t}, \tag{9}$$

where A_{j} and ζ_{j} are the Fourier coefficient for the jth mode and $[k^2(x)+(j\pi/L_1)^2]^{1/2}$, respectively. From Eqs. (4), (8), and (9), the following equation is obtained:

$$i\omega W(x)\eta(x,y) = -\sum_{\mathrm{j}=0}^{\infty} A_{\mathrm{j}}\zeta_{\mathrm{j}} \sinh\left(\zeta_{\mathrm{j}} L_2\right) \cos\left(\frac{j\pi}{L_1} y\right). \tag{10}$$

Using the orthogonality of the cosine function, A_{j} is calculated as

$$A_{\mathrm{j}} = -\frac{i\omega W(x)\int_{-b(x)/2}^{b(x)/2} \eta(x,y)\cos\left(j\pi y / L_1\right)dy}{\zeta_{\mathrm{j}} \sinh\left(\zeta_{\mathrm{j}} L_2\right)\int_{-L_1/2}^{L_1/2} \cos^2\left(j\pi y / L_1\right)dy}. \tag{11}$$

Using the boundary of integration from -$b(x)$/2 to +$b(x)$/2 with respect to y, the following *eikonal equation* is obtained:

$$\begin{aligned} & f(x,\omega) \\ & = D\Big[k^4(x)\int_{-b(x)/2}^{b(x)/2} \eta^2(x,y)dy \\ & - 2k^2(x)\int_{-b(x)/2}^{b(x)/2} \eta(x,y)\partial^2\eta(x,y)/\partial y^2 dy \\ & + [\beta / b(x)]^4 \int_{-b(x)/2}^{b(x)/2} \eta^2(x,y)dy\Big] \\ & - \omega^2\left[\rho_{\mathrm{m}} h\int_{-b(x)/2}^{b(x)/2} \eta^2(x,y)dy + \rho_{\mathrm{l}}\sum_{\mathrm{j}=0}^{\infty} \frac{\left[\int_{-b(x)/2}^{b(x)/2} \eta(x,y)\cos(\mathrm{j}\pi y/L_1)dy\right]^2}{\zeta_{\mathrm{j}} \tanh\left(\zeta_{\mathrm{j}} L_2\right)\int_{-L_1/2}^{L_1/2} \cos^2(\mathrm{j}\pi y/L_1)dy}\right] = 0. \end{aligned} \tag{12}$$

The eikonal equation describes the dispersion relationship between $k(x)$ and ω at various x. The effect of the surrounding fluid is found in the last term of this equation. Since this term contributes to increasing the effective mass of the vibration, the resonant frequency may be decreased by the surrounding fluid. From the average variation principle, it is known that the *eikonal equation* has a relationship with $W(x)$:

$$W(x) = \frac{c}{\left(\frac{\partial f}{\partial k}\right)^{1/2}}, \tag{13}$$

where c is a constant. Eq. (13) is the *transport equation* which describes the qualitative distribution of $W(x)$. Figure 2 shows the graph of envelope curve $W(x)$ in the air environment defined by Eq. (13). In that figure, the peaks at certain frequencies indicate local resonance at a particular place of the ABMP. The peaks of $W(x)$ at each frequency show changing to the smaller x with increasing the frequency of the acoustic wave.

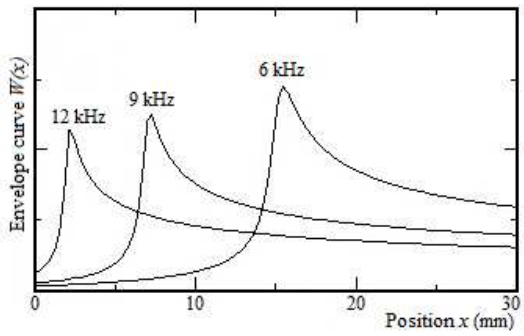

Figure 2 Envelope curve $W(x)$ at 6, 9, and 12 kHz, which is determined on the basis of the analytical solution.

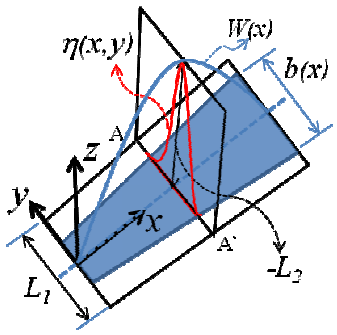

Figure 3 Description of the envelope curve W(x) and a single mode of the vibrating amplitude in y direction η (x, y).

Figure 3 shows the description of the envelope curve *W(x)* and a single mode of the vibrating amplitude in y direction $\eta(x, y)$ at a certain frequency. The maximum vibrating amplitude at a certain frequency L2 occurs at the same place of the local resonance frequency.

4 Experimental Setup

Experiments to realize frequency selectivity have been reported by some researchers. Wittbrodt, *et al.* [6] developed a membrane made of polymide using aluminum beams. Their paper states that this membrane had traveling waves similar to those of the biological basilar membrane. Chen, *et al.* [7] made a membrane by depositing discrete Cu beams on a piezo membrane. They also simulated a membrane using a computational model of the mechanical device. Tanaka, *et al.* [8] developed an acoustic sensor using "*fishbone"* method as a cantilever arrays which realized the frequency selectivity. White, *et al*. [9] developed a membrane made of polymide with Si_3N_4 beams.

There are 24 electrodes on the membrane of the ABMP. These electrodes are used to measure the membrane voltage. We measured the membrane vibration along the whole membrane at the middle of each electrode. Figure 4 shows a diagram of the experimental setup: (a) 3D view and (b) experimental equipment. A sinusoidal acoustic wave was applied to the ABMP via a speaker (FOSTEX, Japan). Previously, the speaker was calibrated to realize a constant sound pressure at various frequencies. The function generator (NF, Japan) connected to the speaker was used to control the frequency of the sound wave of the speaker from 1 to 20 kHz. The speaker was connected in parallel with a signal/function generator and a computer, as shown in Figure 4. We used VBA programming and a UDF, which was inserted in the Excell program to drive the various applied frequencies and sound amplitude to the speaker automatically. We used those frequencies that are within the range of the human audible frequency. An oscilloscope was connected to the speaker in order to analyze the output data sampling at the same time with the input of the various applied frequencies and vibration amplitude of the membrane. The VBA programming and UDF were used to arrange and save the input/output data from a signal/function generator and an oscilloscope. The distance between speaker and membrane was 120 mm. The voltage of the speaker was also adjusted, using a function generator to get a constant sound pressure of 75 dB.

A photograph of the membrane developed in this research is shown in Figure 4(b). The membrane is bonded on the plate with the perforated trapezoid, such that the membrane can easily vibrate by applying an acoustic wave. Although the experiment was done in the atmosphere, both sides of the biological basilar membrane were in lymph fluid. However, the main purpose of this paper is to

understand the basic mechanism of frequency selectivity. In this research, we have used a prototype membrane made of PVDF. The affect and position of the excitation of the membrane are needed to develop a membrane made of P(VDF-TrFE) in the future.

The ABMP was placed on a motorized stage, which could be moved in *x* and *y* directions. The motorized stage was used to examine the spatial distribution of the vibrating amplitude on the surface of ABMP automatically. The vibrating amplitude of the ABMP in z direction was measured by a laser Doppler vibrometer (LDV) (Graphtec, Japan). Using the LDV, the mechanical vibration of the ABMP was converted to velocity data. The velocity data sampling was later analyzed by a Fast Fourier Transform (FFT) using the oscilloscope to obtain a vibration amplitude at the human audible frequency of acoustic waves.

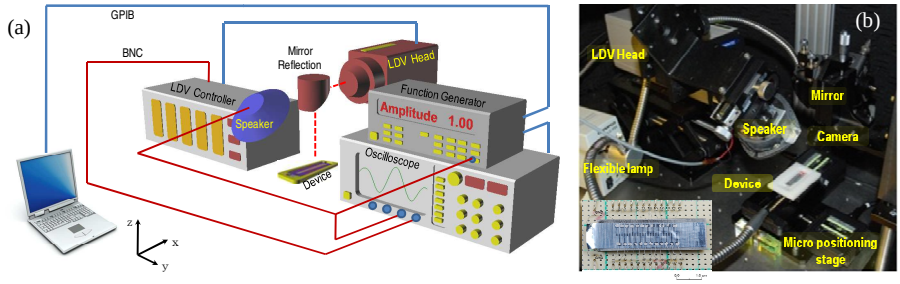

Figure 4 Experimental setup: (a) 3D view and (b) experimental equipment.

The ABMP is relatively large to be directly implanted into the biological cochlea. This problem can be solved by using a micro fabrication method. Optimization and minimization of the membrane remain to be done in a future work.

5 Results and Discussions

The first experiment was done in the atmosphere in order to learn the characteristics of the frequency selectivity mechanism of the prototype membrane. Figure 5 shows a contour map of the vibrating amplitude of the ABMP membrane at f = (a) 6 kHz, (b) 9 kHz, and (c) 12.8 kHz, respectively. These contour maps show the different positions of the maximum amplitude at each frequency. Position x of the maximum amplitudes decreased as the frequency increased.

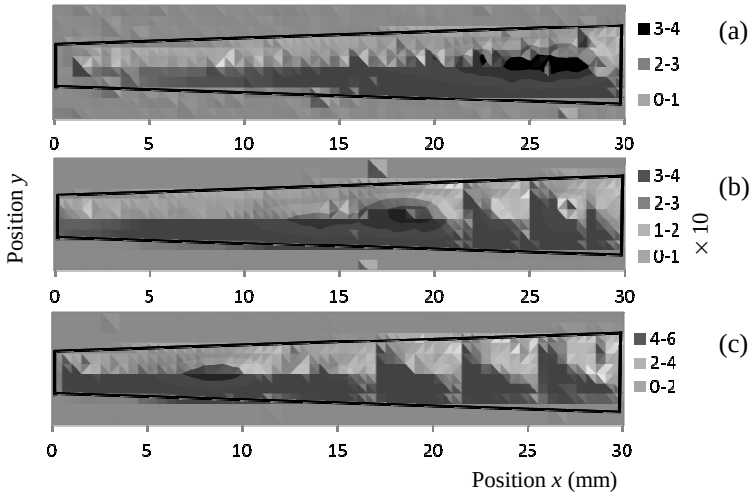

Figure 5 Contour map of the vibrating amplitude of the ABMP membrane at f = (a) 6 kHz, (b) 9 kHz, and (c) 12.8 kHz.

The local maximum amplitudes are considered to be the result of the standing waves in x direction. The maximum vibrating amplitude occurred at the distances x = (a) 27.5 mm, (b) 19 mm, and (c) 8.5 mm from the base, with an amplitude of 36.7 nm, 35 nm, and 54.6 nm, respectively.

Several small peaks were observed at a frequency area lower than the resonance frequency, which was caused by the standing wave. The standing wave was not observed at frequencies higher than the resonating place, which was caused by the fact that the wavelength is relatively long at higher frequencies. Referring to the theory, it is confirmed that the wavelength $k(x)$ is relatively small. In the biological cochlea, the acoustic wave travels from the basal (wider area) to the apex (sharper area). This condition shows that the characteristics of the wave and the oscillation of the prototype membrane are the same as those of the biological membrane.

Figure 6 shows the frequency-dependence of the vibrating amplitude of the ABMP at the distances x = (a) 27.5 mm, (b) 19 mm, and (c) 8.5 mm. The maximum vibrating amplitudes show clear peaks at different frequencies. The frequency at the maximum vibrating amplitude is considered to be the resonant frequency at that local area of the membrane. The maximum frequency increases as the x position decreases. This corresponds to the results in Figure 5. That is, the wavelength of the acoustic wave was affected by the width of the membrane. When the ABMP is relatively wide in x direction compared to the width in y direction, the vibration is mainly effected by the boundary conditions at $y=\pm b(x)/2$. Oscillation of the membrane is dominated by the ABMP's local

structural strain in *y* direction. Furthermore, the vibration in *y* direction is larger than that in *x* direction.

Figure 7 shows the relationship between *x* the length of the membrane and the local resonance frequency, f_l, at 75 dB. The local resonance frequency, f_l, has a value similar to that of frequency *f*. Experimentally, the frequency selectivity of the membrane output is induced by the local resonance of the displacement of the membrane. The local resonance frequency, f_l, decreases from 14 to 3 kHz with the increase of position *x* of the membrane length. The local resonance frequencies of the membrane at the positions of *x* were outside of the range of the resonance frequency linetheory. Almost all experimental results were slightly lower than the predictions. Perhaps this is due, firstly, to the fabrication process (effects from photolithography and etching), after which the density of the membrane has changed, and secondly, to an underestimation of Young modulus E. In the literature, E is widely distributed as 3.0~11.0 GPa.

The resonance frequencies of the theoretical analysis predict that the frequency range can be controlled by changing the thickness, density, Young modulus and length of the membrane. Figure 7 also shows frequency *f* compared with the theoretical resonance frequency, f_l, based on the plate bending theory that is solved with the WKB asymptotic method. Agreement between the experimental results and the theoretical analysis was confirmed.

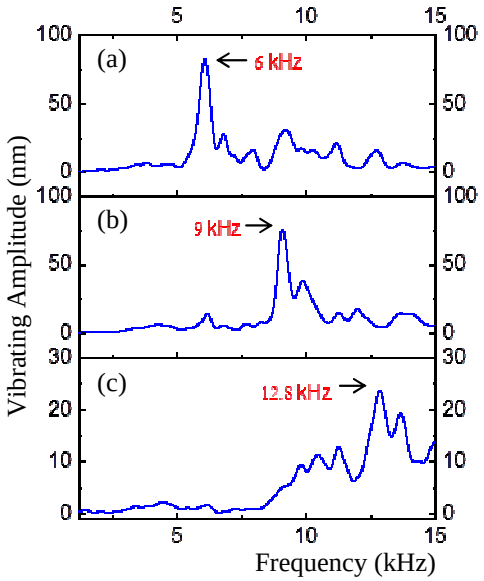

Figure 6 Frequency dependence of the vibrating amplitude of the ABMP at the distances x = (a) 27.5 mm, (b) 19 mm, and (c) 8.5 mm.

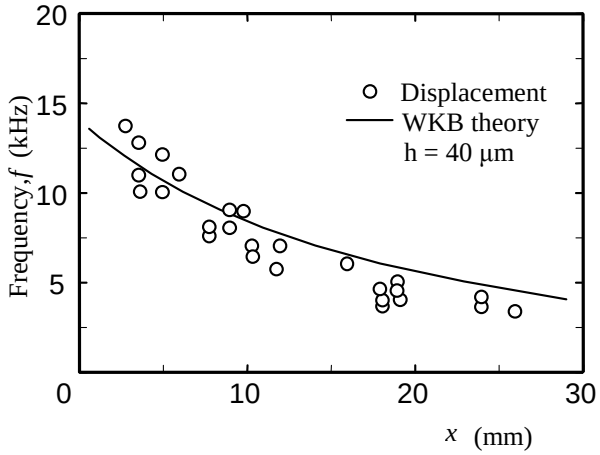

Figure 7 Relationship between the length of the membrane (x) and the local resonance frequency (f) at 5 dB.

6 Conclusions

We have presented an analytical and experimental investigation of our artificial basilar membrane prototype (ABMP). Frequency selectivity of the membrane is confirmed at the range of 3 ~ 14 kHz. The resonant frequency increases as the width of the membrane decreases. Using theoretical calculation, we can predict the thickness of a suitable membrane to be fabricated. Agreement between the experimental data and the theoretical analysis was confirmed. Some of the experimental results were not the same as, or out of the range of the theoretically predicted values. This can be explained by the fabrication process of the membrane and underestimation of the Young Modulus E.

Future work is needed to make the artificial cochlea better as an acoustic sensor. The phase of the oscillations was neglected in this research, since the goal in this experiment was to confirm the frequency selectivity of the prototype membrane. The phase can refer to a specific references of wave and it will be useful to use P(VDF-TrFE) as the material in the next work. The voltage of the artificial auditory membrane is our end goal.The effect of viscosity may also contribute to improve the frequency selectivity of the membrane. Material and fabrication process influence the characteristics of the membrane. We need to minimize the membrane, because the present membrane is relatively large for implantation into a cochlea. A thinner membrane has a vibration amplitude larger than a thicker one, it is relation with the thinner membrane can generate the bigger voltage.

Acknowledgements

The author would like to thank the reviewers for their relevant comments, and special thanks are due to Dr. Yoichi Kagaya and all members of the Kawano Laboratory at the Mechanical Science and Bioengineering Department, Osaka University, Japan.

References

[1] Békésy, von G., *Current Status of Theories of Hearing,* Science, **123**(3201), pp. 779-783, 1956.

[1] Békésy, von G., *Experiments in Hearing*, McGraw Hill, New York, 1960.

[2] Steele, Charles R. & Taber, Larry A., *Comparison of WKB Calculations and Experimental Results for Three-Dimensional Cochlear Models*, J. Acoustical Society of America, **65**(4), April 1979.

[3] Zhou, G., Bintz, L., Anderson, D.Z. & Bright, K.E., *A Life-sized Physical Model of the Human Cochlea with Optical Holographic Readout*, J. Acoust. Soc. Am., **93**(3), pp.1516-1523, 1994.

[4] Ventzel, Eduard & Krauthammer, Theodor, *Thin Plates and Shells: Theory, Analysis, and Applications*, Marcel Dekker, Inc., New York, USA, 2001.

[5] Whitham, G.B., *Linear and Nonlinear Waves*, Wiley-Interscience, 1974.

[6] Wittbrodt, M., Puria, S. & Steele, C.R., *Developing a Physical Model of the Human Cochlea Using Micro-fabrication Methods*, Audiology and Neurotology, **11**(2), pp.104-112, 2006.

[7] Chen, F., Cohen, H., Bifano, T.G., Castle, J., Fortin, J., Kapusta, C., Mountain, D.C., Zosuls, A. & Hubbar, A.E., *A Hydromechanical Biomimetic Cochlea: Experiments and Models*, J. Acoust. Soc. Am., **119**(1), pp. 394-405, 2006.

[8] Tanaka, K., Abe, M. & Ando, S., *A Novel Mechanical Cochlea "fishbone" with Dual Sensor/Actuator Charateristics*, IEEE/ASME Transactions on Mechatronics, **3**(2), pp.98-105, 1998.

[9] White, R.D. & Grosh, K., *Microengineered Hydromechanical Cochlear Model*, Proceedings of the National Academy of Sciences of the United States of America, **102**(5), pp.1296-1301, 2005.